J-Q APROACH FOR CLEAVAGE FRACTURE IN DIFFERENT STRUCTURAL COMPONENTS.

Sebastian Cravero
Fracture Mechanics and Structural Integrity Group - NVFRAC
Dept. of Naval Architecture and Ocean Eng., University of São Paulo
E-mail: sebastian.cravero@poli.usp.br

Claudio Ruggieri
Fracture Mechanics and Structural Integrity Group - NVFRAC
Dept. of Naval Architecture and Ocean Eng., University of São Paulo
E-mail: claudio.ruggieri@poli.usp.br

Abstract: Cracked structural bodies with shallow flaws are shown to lose J dominance. The loss of single parameter characterization is associated with the development of plasticity due to nearby free-stress cracked faces. This loss of J dominance is characterized by the Q parameter. The J-Q theory provides a concise framework to correlate toughness data as a function of constraint and to utilize such data in engineering applications. The J integral sets the size scale over which large stresses and strains develop while Q,, scales the near-tip stress ahead of the crack tip. An introduction to the J-Q methodology is given. J-Q curves obtained from finite elements analyses for different fracture specimens and pipes containing flaws are compared. Furthermore, the effects of crack size and specimen type on fracture are addressed.

Keywords. *cleavage fracture, stress triaxiality, Q parameter*

1. Introduction

Conventional fracture mechanics methodologies to assess the unstable cracking behavior (cleavage fracture) of different cracked bodies (i.e., laboratory specimens and engineering structures) rely on the similarity of their respective crack-tip stress and deformation fields as schematically illustrated in Fig. (1). Under small scale yielding (SSY) conditions, a single parameter, such as the linear elastic stress intensity factor, *K*, and the *J*-integral (or, equivalently, the crack tip opening displacement, *CTOD* or δ), uniquely scales the elastic-plastic near-tip fields. In the present context, SSY is meant to pertain to loading conditions for which near-tip plasticity is well contained and controlled by the elastic fields for an infinite crack. To the extent that such one parameter singular fields dominate over microstructurally significant size scales (i.e., the fracture process zone (FPZ) of a few *CTOD*s ahead of a macroscopic crack), parameters (*K* and *J*) (δ) fully describe the local condition leading to unstable (cleavage) failure (Hutchinson, 1983). However, fracture testing of ferritic structural steels in the ductile-to-brittle (DBT) transition region consistently reveals a significant effect of specimen geometry and loading mode (bending vs. tension) on cleavage toughness values as measured by the critical parameters K_{Ic}, J_c or δ_c, (De Castro et al., 1979 and Sorem et al., 1991, for illustrative data). These studies show significant elevations in the elastic-plastic fracture toughness for shallow cracked SE(B) specimens and tension geometries of ferritic steels tested in the transition region, where transgranular cleavage triggers macroscopic fracture. At increased loads in a finite body, such as a cracked specimen or structure, the initially strong SSY fields gradually change to fields under large scale yielding (LSY) as crack tip plastic zones increasingly merge with the global bending plasticity on the nearby traction free boundaries. This phenomenon, often termed *loss of crack tip constraint*, contributes to the *apparent* increased toughness of shallow cracked and tension loaded geometries observed in fracture testing. Once SSY conditions no longer apply, larger *J*-values in the finite body are necessary to generate a highly stressed region ahead of crack tip sufficient to trigger cleavage. These features have enormous practical implications in defect assessment procedures, particularly repair decisions and life extension programs of in-service structures as well as structural design specifications.

The above limitations of single parameter fracture mechanics approaches motivated research efforts to characterize the complex interaction of crack tip separation processes with global loading, geometry and material flow properties using two-parameter fracture theories. The two-parameter *J-T* and *J-Q* theories (Betegon, et. al., 1991 and O'Dowd and Shih, 1991) extend a fundamental concept of fracture mechanics associated with the use of scalar parameters to quantify the strain-stress fields ahead of a stationary crack tip. Within these methodologies, the *J*-integral sets the size scale over which high stresses develop while the second parameter (*T, Q*) quantifies the level of stress triaxiality at distances of a few *CTODs* ahead of the crack tip. The addition of a second parameter (*T, Q…*) leads to the construction of experimentally derived fracture toughness loci, rather than conventional, single-valued definitions of toughness. The correlation of fracture conditions across different crack geometries/loading models for the same material (and temperature) then proceeds without recourse to detailed features of the crack tip separation processes. At identical values of the scalar parameters (*J, Q, T…),* the crack tip strain-stress fields that drive the local fracture have identical values as well. Efforts adopting this approach focus primarily on cleavage fracture under large-scale yielding prior to significant ductile tearing.

The objectives of this brief paper focus on a summary of a correlative approach based on the *Q*-parameter to characterize constraint effects on cleavage fracture toughness. Discussions emphasize features of representative 2-D numerical analyses of different cracked specimens and longitudinally cracked pipes. The plan of the article is as follows. The next section discusses the notion of constraint and the utility of small scale yielding reference solutions. This is followed by a very brief description of the *J-Q* approach which extends correlative fracture mechanics beyond the limits given by *SSY* conditions. *J-Q* trajectories for different crack test specimen geometries including a conventional C(T) specimen and a SE(T) crack configuration, are presented and correlated with numerical results for the cracked pipe. A significant similitude between the SE(T), shallow cracked SE(B) specimens and the axial external cracked pipe is found. Moreover, the variation of parameter *Q* ahead of crack-tip is analyzed to validate its utility in characterizing the stress field in this region.

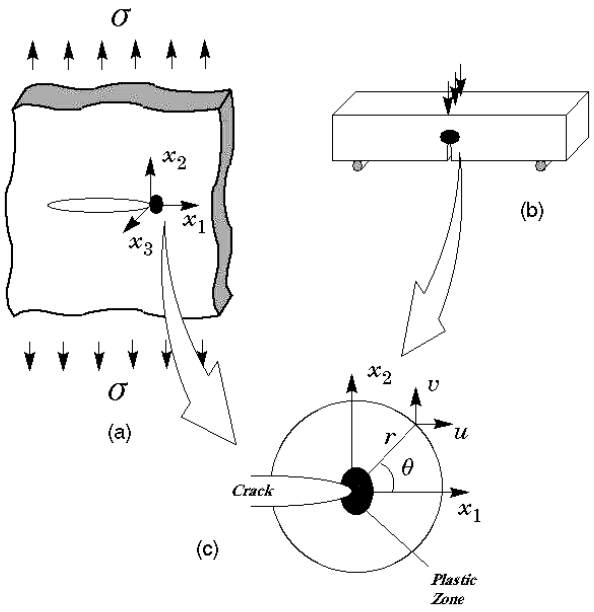

Figure 1: Schematic illustration of the validity of the single parameter approach. The crack-tip conditions should be identical in the structural component (a) and the fracture specimen (b), as long as the plastic zone (c) is small.

Crack-Tip Constraint and SSY

Constraint most generally refers to the evolving level of stress triaxiality ahead of the crack front under increased remote loading. In a specimen with finite dimensions, the boundary conditions strongly affect the crack-tip stress-strain fields. The stresses are generally lower than the stresses in an infinite cracked body. This phenomenon is often known as *loss of crack tip constraint.* When comparing differences in constraint between crack configurations, questions arise about the precise definition of stress triaxiality and about the relevant position(s) ahead of the crack front at which such comparisons are made. The most common theories to characterize the loss of crack-tip constraint are the *J-T* and *J-Q* methodologies; they compare the stress fields computed for finite bodies with a reference field constructed for small-scale yielding (SSY) conditions. To compute the constraint loss, the stress fields in the finite body is compared with the field for a reference solution. Commonly the reference solution is obtained from a finite elements analysis of a "*Modify Boundary Layer"* (MBL) model (Larsson and Carlsson, 1973 and Rice, 1974). The MBL model enables the construction of *SSY* fields for general material response. Figure (2) shows a plane-strain element mesh which represents a single-ended crack in an infinite body. Specified values for K_I and T applied on this model uniquely define the linear elastic remote field enclosing a vanishing small plastic zone at the tip (i.e., compared to the finite extent of the finite mesh). To obtain the boundary condition displacements imposed on the model, we use the first two terms of the asymptotic Mode I Williams solution (Williams, 1957) to obtain elastic displacements in the form

$$u(R,\theta) = K_I \frac{1+\nu}{E}\sqrt{\frac{R}{2\pi}}\cos\left(\frac{\theta}{2}\right)(3-4\nu-\cos\theta)+T\frac{1-\nu^2}{E}R\cos\theta$$
$$v(R,\theta) = K_I \frac{1+\nu}{E}\sqrt{\frac{R}{2\pi}}\operatorname{sen}\left(\frac{\theta}{2}\right)(3-4\nu-\cos\theta)+T\frac{\nu(1+\nu)}{E}R\operatorname{sen}\theta \quad (1)$$

where u and v are the displacements in the x_1 and x_2 direction respectively, R and θ are polar coordinates centered at the crack-tip with $\theta = 0$ corresponding to a line ahead of the crack tip, E is the Young's modulus and ν is Poisson's ratio.

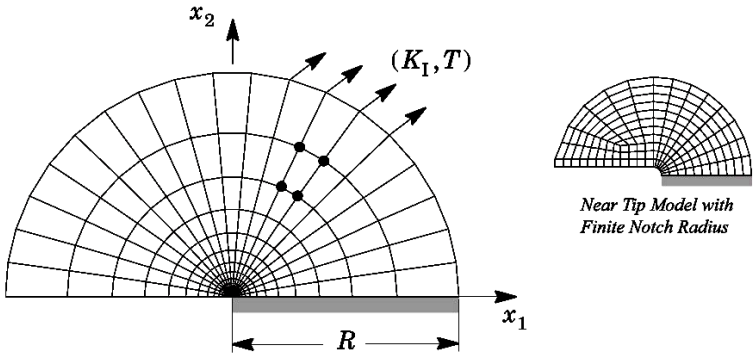

Figure 2: *MBL* Finite Element Model.

J-Q Theory

The characteristic feature emerging from a multi-parameter description of the (stationary) elastic-plastic crack tip fields in homogeneous materials is the use of a scalar parameter to quantify the magnitude of these fields. Here the J-integral sets the size scale over which high stresses develop while the second parameter (the elastic T-stress or the hydrostatic Q-parameter) quantifies the level of stress triaxiality at distances of a few *CTODs* ahead of the crack tip. In particular, the J-Q description of mode I, plane strain crack tip fields derives from considerations of a modified boundary layer (MBL) formulation in which the remote tractions are given by the first two-terms of William's linear elastic solution

$$\sigma_{ij} = \frac{K_I}{\sqrt{2\pi r}} f_{ij}(\theta) + T\delta_{1i}\delta_{1j} . \tag{2}$$

Crack tip fields differing in stress triaxiality are generated by varying the non-singular T stress, parallel to the crack plane (which does not affect the value of J). From dimensional considerations, these fields can be represented by a family of self-similar fields parameterized by the load parameter T/σ_0 which provides a convenient measure of near-tip stress triaxiality such as, for example, when assessing effects of specimen geometry on crack tip constraint (Dodds et. al., 1993). However, the general applicability of T under fully yielded conditions become elusive since the elastic solution given by Eq. (2), upon which the T-stress is defined, is an asymptotic solution which is increasingly violated as plastic flow progresses beyond well contained near tip yielding.

The above limitations motivated O'Dowd and Shih (1991, 1992) to propose an *approximate* two-parameter description for the elastic-plastic crack-tip fields based upon a triaxiality parameter more applicable under LSY conditions for materials with elastic-plastic response described by a power hardening law given as

$$\begin{aligned} \varepsilon/\varepsilon_0 &= \sigma/\sigma_0 , \qquad \varepsilon_0 \le \varepsilon \\ \varepsilon/\varepsilon_0 &= \left(\sigma/\sigma_0\right)^n , \qquad \varepsilon_0 > \varepsilon \end{aligned} \tag{3}$$

Here, n denotes the strain hardening exponent, σ_0 and ε_0 are the reference (yield) stress and strain, respectively. Guided by detailed numerical analyses employing the MBL model O'Dowd and Shih (1991) identified a family of self-similar fields in the form of

$$\sigma_{ij} = \sigma_0 \hat{f}_{ij}\left(\frac{r}{J/\sigma_0}, \theta, Q\right) \tag{4}$$

where the dimensionless second parameter defines the amount by which σ_{ij} in fracture specimens differ from the reference *SSY* solution with $T=0$.

Limiting attention to the forward sector ahead of the crack tip between the $SSY_{T=0}$ reference solution and the fracture specimen field, O'Dowd and Shih (1991) showed that $Q\sigma_0$ corresponds effectively to a spatial uniform hydrostatic stress, i.e., the d*ifference* field relative to a high triaxiality reference stress state

$$\sigma_{ij} = (\sigma_{ij})_{SSY;T=0} + Q\,\delta_{1i}\delta_{1j}\,; \quad |\theta| < \frac{\pi}{2}, \quad J/\sigma_0 < r < 5\,J/\sigma_0\,. \tag{5}$$

Operationally, Q is defined by

$$Q \equiv \frac{\sigma_{\theta\theta}^{FB} - \sigma_{\theta\theta}^{SSY;T=0}}{\sigma_0}; \quad at:\ \theta = 0, \quad r = \frac{2J}{\sigma_0} \tag{6}$$

where finite element analyses containing sufficient mesh refinement to resolve the fields at this length scale provide the finite body stresses. Here, we note that Q is evaluated at $r = 2J/\sigma_0$ for definiteness; however, O'Dowd and Shih (1991) also showed that Q is virtually independent of distance in the range $J/\sigma_0 < r < 5J/\sigma_0$.

Construction of a *J-Q* trajectory follows by evaluation of Eq. (6) at each stage of loading in the finite body. This procedure imposes no restrictions on models to describe material flow properties or incremental *vs.* deformation plasticity. Large geometry change (*LGC*) may be included although values of Q derived form small geometry change (*SGC*) analyses prove satisfactory in applications which make use of stresses sufficiently outside the near tip blunting region. Figure (3) qualitatively compares the crack-tip constraint levels defined by Q for different geometries and shows that the shallow crack specimens and axially flawed pipes appear to have similar crack-tip constraint. In particular the cracked pipe displays very low levels of constraint compared to common test specimens (e.g. C(T) and deeply cracked SE(B) specimens). This behavior produces an "apparent" increase in fracture toughness which may lead to an excessive conservatism in common fracture assessment procedures. This conservatism could be avoided by using test specimen geometries that present similar constraint behavior to the cracked pipes as will be presented later.

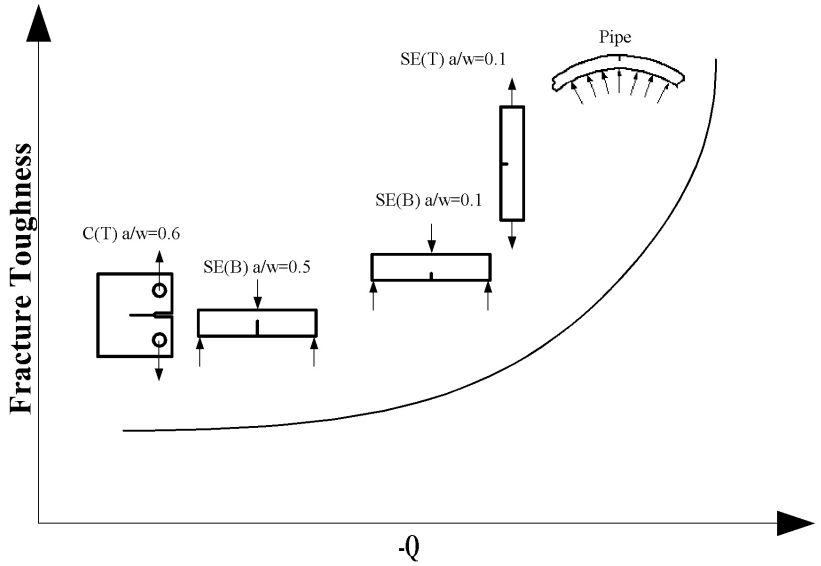

Figure 3: Qualitative comparison of the crack-tip constraint levels vs. fracture toughness for different geometries.

Computational Models

2-D numerical analyses were conducted for conventional fracture specimens and a longitudinally cracked pipe. The matriz analyses include a compact tension C(T) specimen with a/W=0.6, a single edge notched SE(B) specimen under bending with a/W=0.5 and a/W=0.1, and a single edge notched SE(T) specimen under tension with a/W=0.1. Here, a is the crack length and W is the specimen width as illustrated in Fig. (4). The specimen dimensions are shown in Table (1). The cracked pipe has external diameter D=508 mm (20") and wall thickness t=12.7 mm with a/t=0.1, 0.25 and 0.5. In all analyses, the material considered has the following characteristics: $n = 10$, $E/\sigma_0 = 500$ and $\nu = 0.3$; where, n denotes the strain hardening exponent corresponding to a Ramberg-Osgood power hardening law, σ_0 and ε_0 are the reference (yield) stress and strain, respectively. These mechanical properties represent common pressure vessel and pipe steels.

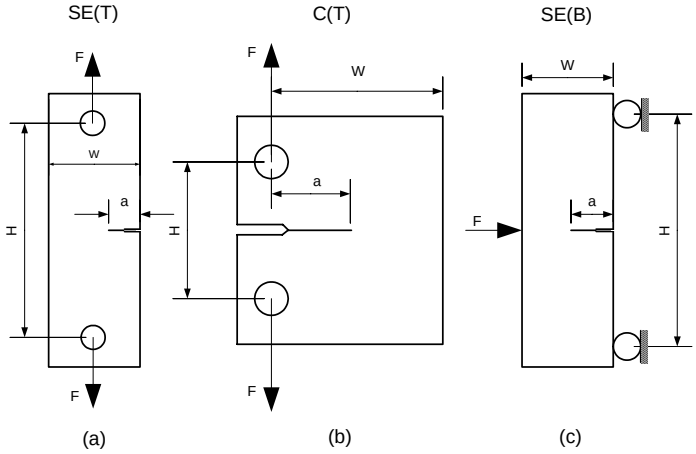

Figure 4: Test Specimens Geometries.

Table 1: Specimens Principal Dimensions.

	C(T) a/W = 0.6	SE(B) a/W = 0.5	SE(B) a/W = 0.1	SE(T) a/W = 0.1
W	50.8 mm	50.8 mm	50.8 mm	50.8 mm
H	61 mm	203.2 mm	203.2 mm	203.2 mm

Figure (5) shows the finite element meshes for the different crack configurations used in this work. A conventional mesh configuration having a focused ring of elements surrounding the crack front is used with a small key-hole at the crack tip; the radius of the key-hole, ρ_0, is 25 μm (0.0025mm). Symmetry conditions enable analyses using one-half of the 2-D models with appropriate constraints imposed on the symmetry planes. The half-symmetric models typically have 1500-2000 elements. The computations reported here are generated using the non-linear code WARP3D (Koppenhoefer et. al., 1994) which implements the Mises constitutive model in a small strain setting. Evaluation of the *J*-integral employs a domain integral procedure (Moran et. al., 1987) which computes values for *J* over domains defined outside the material having highly non-proportional history of the near-tip fields. These *J*-values provide a convenient parameter to characterize the intensity of far field loading on the crack front. The *J*-*Q* trajectories are computed by using the research code JQCRACK (Cravero and Ruggieri, 2003) which processes the stresses from the finite body model and the MBL model to obtain the *Q* parameter as a function of *J*.

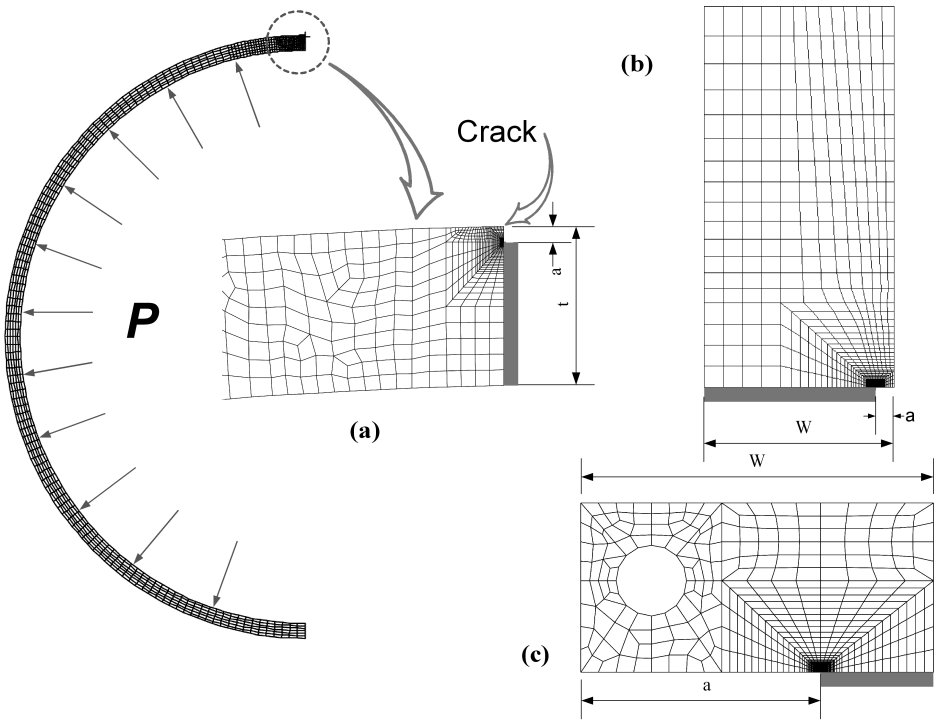

Figure 5: 2-D meshes (a) 20” Pipe with a/t = 0.1; (b) SE(T) and SE(B) with a/w = 0.1; (c) C(T) with a/w = 0.6

J-Q Trajectories for Fracture Specimens

Figures (6) to (8) present key results describing the evolution of parameter *Q* with increased loading, as measured by *J*, for the analyzed fracture specimens. Figure (6) shows the *J-Q* trajectories for the different test specimens with the loading parameter, *J*, normalized by $b\sigma_0$ where *b* is the remaining ligament (*W*–*a*). For the deep notch C(T) and SE(B) specimens ($a/W \geq 0.5$), the *Q*-parameter remains within the range $-0.2\sigma_0$ to $0.2\sigma_0$ for the entire loading which indicates that the global geometry does not have a very significant effect on the stress level compared to the reference MBL solution. Consequently, these specimens can be regarded as high constraint geometries within the present context. In contrast, the shallow crack SE(B) and SE(T) specimens display a significant loss of crack-tip constraint as measured by decreased levels of parameter *Q* even earlier in the loading; here the *Q*-parameter remains beyond the values of –0.8 for almost the entire range of loading.

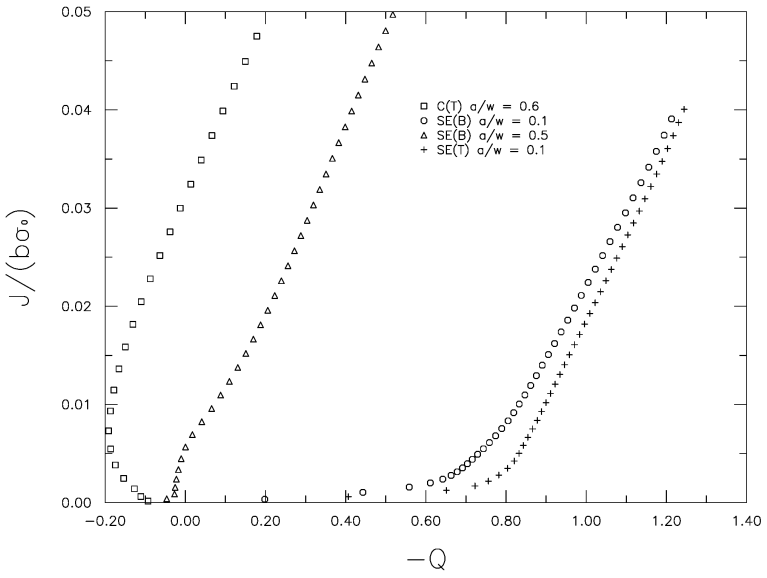

Figure 6: *J-Q* trajectories for different test specimens.

Figures. (7) and (8) show the *Q* variation with normalized distances ahead of crack tip for the analyzed specimens. Finite strain effects dominate for $r/(J/\sigma_0) < 1$, while terms of higher order than *Q* can be significant at large normalized distances. Consequently, it is important to analyze the dependency of parameter *Q* for the interval $1 < r/(J/\sigma_0) < 5$ (recall that the *Q*-values are evaluated at $r/(J/\sigma_0)=2$ in the present work). These figures show a weak dependence of *Q* on normalized distance $r/(J/\sigma_0)$ for the shallow crack configurations (SE(B) and SE(T) specimens with $a/W=0.1$) for different load levels. Parameter *Q* also displays a weak dependence on $r/(J/\sigma_0)$ for the deep crack configurations (C(T) with $a/W=0.6$ and SE(B) with $a/W=0.5$) but only for lower load levels. At higher loading in these specimens, the *Q*-value variation ahead of crack tip is more pronounced.

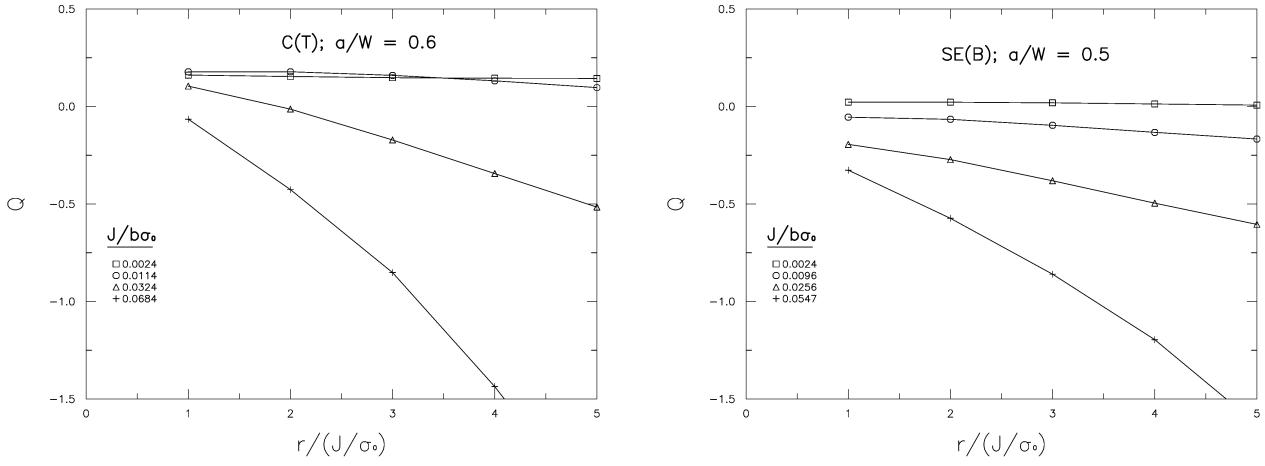

Figure 7: Dependence of *Q* on normalized distance ahead of crack tip for C(T) with $a/W = 0.6$ and SE(B) with $a/W = 0.5$

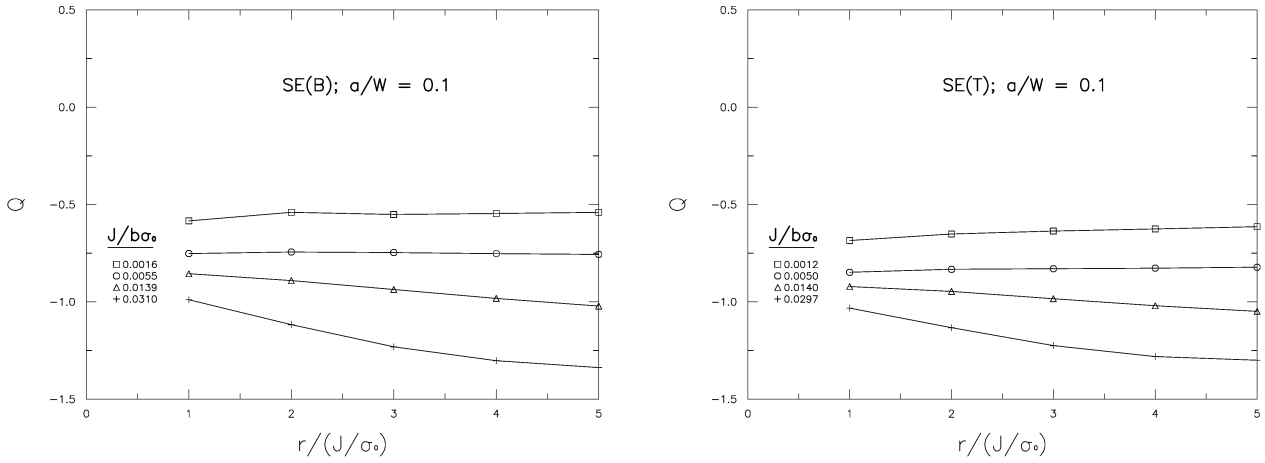

Figure 8: Dependence of *Q* on distance ahead of crack tip for SE(B) with *a/W* = 0.1 and SE(T) with a/W = 0.1

J-*Q* Trajectories for the Cracked Pipe

Figures (9) to (11) present key results describing the evolution of parameter *Q* with increased loading, as characterized by *J*, normalized by $b\sigma_0$ where *b* is the remaining ligament (*t*–*a*), for the analyzed flawed pipe. Figure (9) provides the *J*-*Q* trajectories constructed for the cracked pipes with *a*/*t*=0.1, 0.25 and 0.5. The plot shows a strong effect of crack depth on the levels of crack-tip stress triaxiality as measured by parameter *Q*. In particular, the loss of crack-tip constraint is very pronounced for the cracked pipes with *a*/*t*=0.1 and 0.25 even at very low load levels. The variation of the *Q*-value throughout the normalized crack tip distance is plotted in Figs. (10) and (11). These figures show that the *Q*-values are essentially constant in the shallow cracked pipes whereas for the deeply cracked pipe there is a more pronounced dependence of parameter *Q* on crack-tip distance particularly at higher deformation levels. Here, this effect most likely arises due to the high *a*/*t*-ratio coupled with the thin wall for this pipe. Because parameter *Q* is evaluated at a fixed nondimensional distance, the higher loads on this pipe cause the stresses to be measured at regions very close to the internal pipe surface. The free surface in the internal pipe relaxes the near-tip stresses and, consequently, affects the computed *Q*-values.

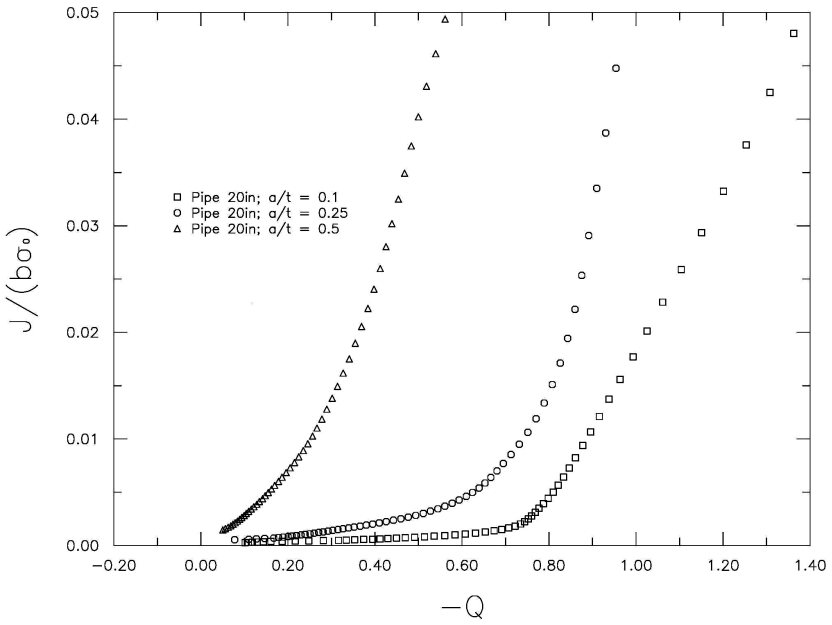

Figure 9: *J*-*Q* trajectories for longitudinally cracked pipes with different *a*/*t*-ratios.

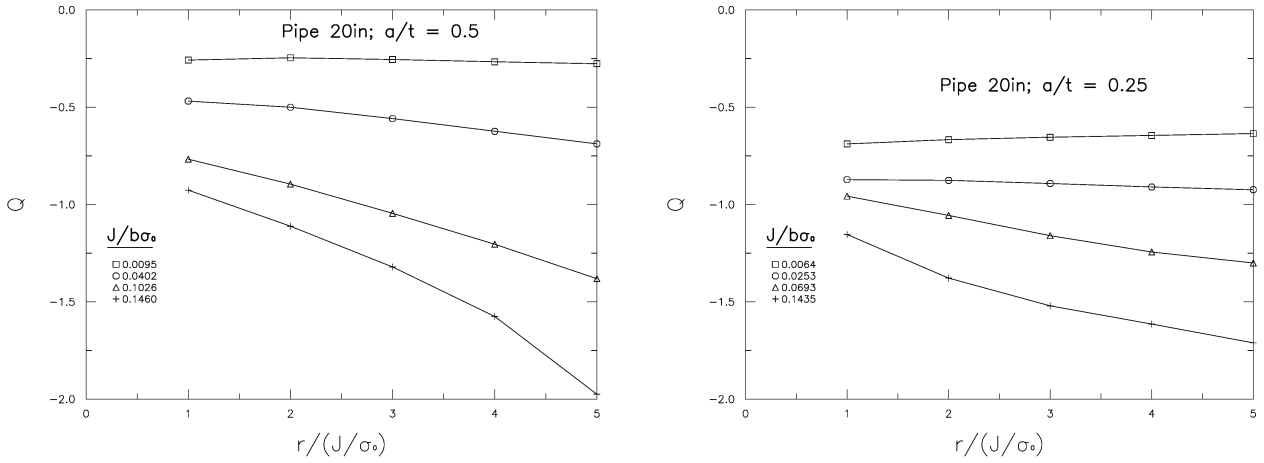

Figure 10: Dependence of Q on nondimensional crack-tip distance for the cracked pipes with for a/t = 0.5, a/t = 0.25

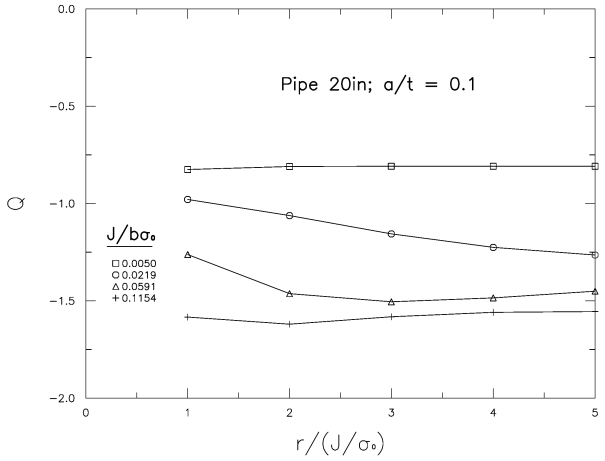

Figure 11: Dependence of Q on nondimensional crack-tip distance for cracked pipe with a/t = 0.1

Comparison of *J*-*Q* Trajectories for Shallow Crack Specimens and the Cracked Pipe.

Figure (12) compares the *J*-*Q* trajectories for the shallow crack SE(B) and SE(T) specimens (a/W=0.1) and the cracked pipe with a/t=0.1. The results demonstrate that the evolution of parameter Q with J is essentially similar for these fracture specimens and the cracked pipe for the entire range of loading. Within the present two-parameter methodology, the correlation of fracture conditions across these crack configurations can simply be made by specifying the loading parameter J and the stress triaxiality Q. Moreover, these results also show important implications for defect assessment of shallow cracked pipes. Use of shallow cracked SE(B) or SE(T) specimens does provide a much better characterization of the crack tip conditions for a longitudinal flaw in a pipe than the widely employed deeply cracked C(T) and SE(B) specimens in standard fracture assessment procedures.

Concluding Remarks

The arguments presented in this brief paper, derived by extensive experimental observations, that conventional fracture mechanic approaches do not suffice to characterize the fracture behavior of fully yielded solids provide a compelling support to develop more realistic methodologies. The *J*-*Q* methodology is a useful procedure for structural integrity assessment for low constraint structural components. Exploratory analyses of common 2-D fracture specimens have shown a significant effect of crack depth on the *J*-*Q* trajectories for these crack configurations. The results demonstrate that shallow crack specimens display a significant loss of crack-tip constraint even at low deformation levels. *J*-*Q* trajectories computed for longitudinally cracked pipes with different crack depth to wall thickness (a/t) ratio also display strong similarities with corresponding trajectories for the shallow crack configurations. The methodology thus appears to provide significant improvements in defect assessment procedures to predict failure in longitudinally

cracked pipes. Further work is currently underway to validate the use of SE(T) specimens in structural integrity procedures applicable to defect assessments in oil and gas pipelines and pressure vessels.

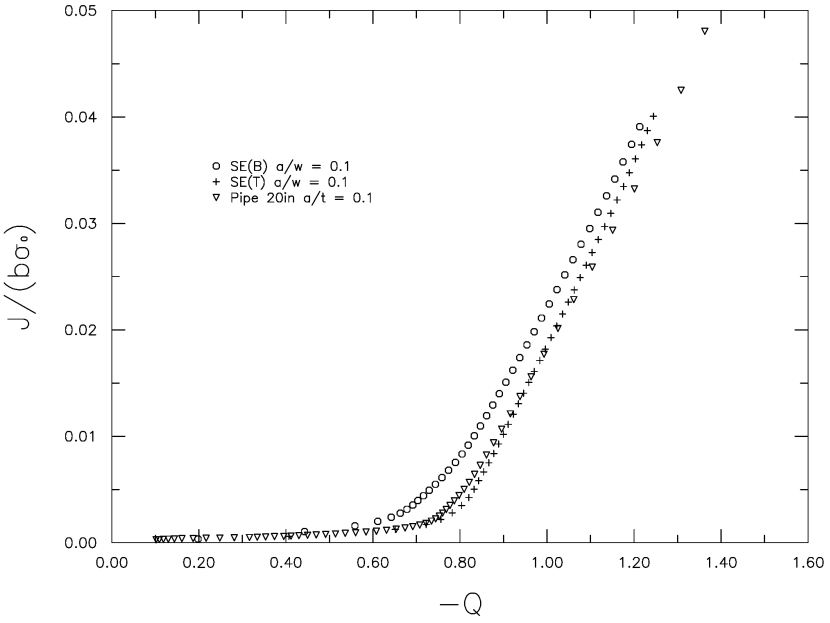

Figure 12: *J*-*Q* curves for the cracked pipe with *a*/*t*=0.1 and shallow cracked specimens

Acknowledges

This investigation was supported by principally from the Scientific Foundation of the State of São Paulo (FAPESP) under grant 01/06919-9 and 02/06328-3 and by the National Council of Scientific and Technological Development – CNPq (Grant: PQ 300048/97-1).

References

Betegon, C., and Hancock, J. W., 1991, "Two-Parameter Characterization of Elastic-Plastic Crack Tip Fields.", Journal of Applied Mechanics, Vol. 58, pp. 104-113.

Cravero, S., Ruggieri C., 2003, "JQCRACK Versão 1.0 Cálculo Numérico do Parâmetro Hidrostático Q para componentes Estruturais 2D Contendo Trinca." Boletim Técnico da Escola Politécnica da Universidade de São Paulo, Departamento de Engenharia Naval e Oceânica, BT/PNV/59, (in Portuguese).

De Castro, P.M.S.T., Supurrire, J., Hancock, P., 1979, "An Experimental Study of the crack length/specimen width (a/W) ratio dependence of the crack opening displacemnt (COD) test using small-scale specimens." Fracture Mechanics, ASTM STP 677 (Smith, C. W., Ed.), American Society for Testing and Materials, pp. 486-497.

Dodds R. H. Jr.. Shih, C. F. and Anderson, T. L., 1993, "Continuum and Micro-mechanics Treatment of Constraint in Fracture", International Journal of Fracture, Vol. 64, pp. 101-133.

Hutchinson, J. W., 1983, "Fundamentals of the Phenomenological Theory of Nonlinear fracture Mechanics.", Journal of Aplied Mechanics, Vol. 50, pp. 1042-1051.

Koppenhoefer, K., Gullerud, A., Ruggieri, C., Dodds, R. and Healy, B., 1994, "WARP3D: Dynamic Non-linear Analysis of Solids Using Preconditioned Conjugated Gradient Software Architecture.", Structural Research Series (SRS) 596, UILU-ENG-94-2017, University of Illinois at Urbana Champaign.

Larsson, S. G. and Carlsson, A. J., 1973, "Influence of Non-Singular Stress Terms and Specimen Geometry on Small Scale Yielding at Crack-Tip in Elastic-Plastic Materials.", Journal of Mechanics and Physics of Solids, Vol.21., pp. 263-277.

Moran, B. and Shih, C. F., 1987, "A General Treatment of Crack Tip Integrals", International Journal of Fracture, Vol. 35, pp. 295-310.

O'Dowd, N. P., and Shih, C. F., 1991, "Family of Crack-Tip Fields Characterized by Triaxiality Parameter: Part I – Structure of Fields.", Journal of Mechanics and Physics of Solids, Vol.39., No. 8, pp. 989-1015.

O'Dowd, N. P., and Shih, C. F., 1992, "Family of Crack-Tip Fields Characterized by Triaxiality Parameter: Part II – Fracture Aplications.", Journal of Mechanics and Physics of Solids, Vol.40., pp. 939-963.

Rice, J. R., 1974, "limitation of the Small Scale Yielding Approximation for Crack-Tip Plasticity", Journal of Mechanics and Physics of Solids, Vol.22, pp. 17-26.

Sorem, W. A., Doods, R. H., Rolfe, S.T., 1991, "Effects of crack depth on elastic-plastic fracture toughness.", International Journal of Fracture, Vol. 17 (1), pp. 27-43.

Williams, M. L., 1957, "On the Stress Distribution at the Base of a Stationary Crack.", Journal of Applied Mechanics, Vol. 24, pp. 109-114.